NMR Chemical Shielding Surface of *N*-Acetyl-*N*′-Methylalaninamide: A Density Functional Study

HORST M. SULZBACH,[1,2] GEORGE VACEK,[1] PETER R. SCHREINER,[1,2] JOHN MORRISON GALBRAITH,[1] PAUL von R. SCHLEYER,[1,2] and HENRY F. SCHAEFER, III[1,*]

[1] *Center for Computational Quantum Chemistry, University of Georgia, Athens, Georgia 30602-2556*
[2] *Computer Chemistry Center, Institute of Organic Chemistry I, Universität Erlangen–Nürnberg, Henkestrasse 42, D-91054 Erlangen, Germany*

Received 16 November 1995; accepted 14 February 1996

ABSTRACT

The five energetically lowest minima on the potential energy surface of *N*-acetyl-*N*′-methylalaninamide were optimized at the Becke3LYP/DZ*d* level of theory to compare these density functional theory results with the literature findings at restricted Hartree–Fock/3–21G. While the relative energies are very similar, the amide moiety is predicted to be much more flexible at Becke3LYP/DZ*d*. As a consequence, the three minima that favor a nonplanar amide group differ by up to 14° in their ϕ and ψ values between the two levels. To compare the change in the density functional NMR chemical shifts with respect to ϕ and ψ with experimental results, Becke3LYP/DZ*d* was employed to optimize a structure for *N*-acetyl-*N*′-methylalaninamide at each 30° interval on the (ϕ, ψ) surface in the regions that correspond to the α helix and the β-pleated sheet and at each 60° interval elsewhere. The corresponding NMR chemical shielding surface was computed with the density functional program deMon. The resultant NMR chemical shielding surfaces for *N* and C^{β} are in good agreement with the experiment, while the change in the NMR chemical shielding of C′ and C^{α} cannot be described only in terms of ϕ and ψ. The chemical shifts for those atoms also depend on the nonplanarity of the amide moiety. We evaluated this dependence for *N*-methylacetamide as a model system. Estimates of the parameters derived from *N*-methyl-acetamide allowed the NMR-shielding surfaces of C′ and C^{α} to be corrected for the nonplanar nitrogen influence. Although the effect is less pronounced with lower level theoretical geometries, due to the smaller degree of pyramidalization of the amide nitrogen, the (ϕ, ψ)NMR chemical shielding surfaces will need to be

* Author to whom all correspondence should be addressed.

© 1997 by John Wiley & Sons
CCC 0192-8651 / 97 / 010126-13

corrected. The agreement with the experiment was much better for the corrected surface of C′ when the nitrogen in the α helix had a nonplanar environment.
© 1997 by John Wiley & Sons, Inc.

Introduction

The development of FT-NMR and of 2- and 3-dimensional NMR experiments during the past decade has enabled the determination of protein structures in solution.[1] Nuclear-Overhauser enhancement (NOE)[2] between protons located at different regions of the protein is exploited to extract distance information. These distances are then used as constraints in force field calculations to help locate possible protein structures. Although NMR chemical shift information is only used to determine regions where either an α helix or a β-pleated sheet predominates, proteins and peptides are, in principle, ideally suited for structure–NMR-shift correlations. The tertiary structure is dominated by only three angles (ϕ, ψ, and ω) per amino acid residue. Figure 1 shows their definitions for an alanine residue. Because ω refers to the torsional angle C^{α}—C′—N—$C^{\alpha+1}$ around the amide C′—N bond, it is close to 0° for a *cis*-amide linkage and close to 180° for the more common *trans*-amide linkage.[3]

The limited use of NMR chemical shift information is due to the lack of experimental data that correlate the change in the NMR shifts of C^{α}, C^{β}, C′, N, and, to a lesser degree, the hydrogen atoms with the conformation of the peptide. This information is difficult to obtain experimentally because the vast majority of the peptide residues have ϕ and ψ values that correspond to those of an α helix or a β-pleated sheet. Only very few residues in each peptide have backbone dihedral angles with values outside these ''allowed'' areas. Figure 2 shows these allowed regions in a Ramachandran plot.[4] Hence, while it is experimentally known that δ ^{13}C for C^{α} and C′ in an α-helical region are shifted downfield by 2–5 ppm compared to the signals in a β-pleated sheet and δ ^{13}C C^{β} upfield by about the same amount,[5–7] the shift dependence of δ ^{13}C of C^{α}, C′, and C^{β} for other areas of the Ramachandran plot is not known experimentally.

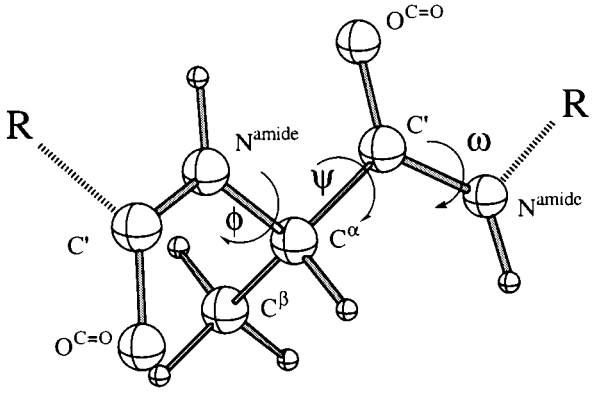

FIGURE 1. Definition of the backbone angles ϕ, ψ and ω, shown for an alanine residue ($\phi = \psi = \omega = 180°$). The dihedral angle C′—N—C^{α}—C′ is designated ϕ and the dihedral angle N—C^{α}—C′—N is designated ψ. The eclipsed conformer has $\phi = 0°$ and $\psi = 0°$. Clockwise rotation is considered positive.

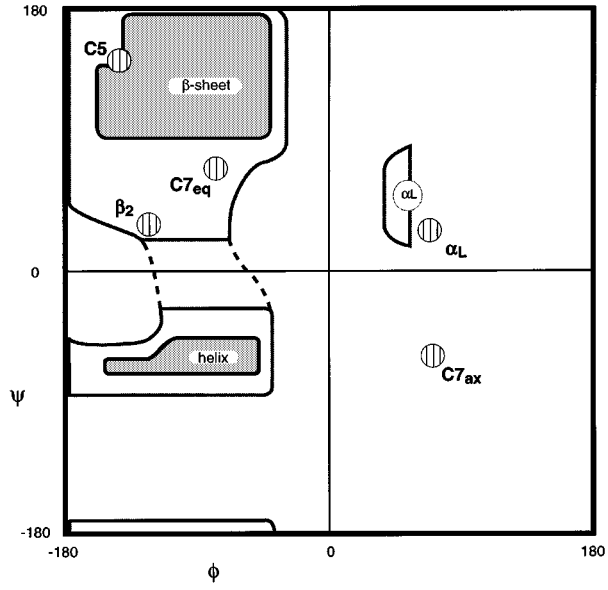

FIGURE 2. Ramachandran plot of the (ϕ, ψ)-surface. The β-sheet region includes the anti-parallel β-sheet and the parallel β-sheet and the helix region includes the right-handed α-helix, the right-handed 3_{10}-helix and the right-handed π-helix. α_L is the left-handed α-helix. The grey areas are lowest in energy, but many residues are still found within the outer borders. The shaded circles correspond to the five lowest minima (**$C7_{eq}$**, **C5**, **$C7_{ax}$**, **β_2** and **α_L**) on the theoretically derived energy surface of *N*-acetyl-*N′*-methylalanineamide. Their structures do not need to correspond to either a helix- or a sheet-like conformation.

The separation of the effect of the backbone dihedrals ϕ and ψ on $\delta\,^{13}C$ from the effect of the side chain dihedral on $\delta\,^{13}C$ constitutes an additional experimental challenge. Finally, only solid-state NMR experiments on peptides or proteins for which an X-ray structure has been previously determined allow an unambiguous correlation between the backbone dihedrals and the NMR chemical shifts. Experimental data based on solution structures are only semiquantitative due to the larger error margin for ϕ and ψ. A large number of residues must be sampled before a reliable correlation between the NMR chemical shifts and the conformation can be deduced.[6,7]

An alternative approach is the *ab initio* computation of the conformational dependencies of the NMR chemical shifts. With the development of fast and accurate algorithms for the theoretical evaluation of the magnetic properties, the computation of NMR chemical shifts is gaining interest rapidly.[8] While the original algorithms, based on IGLO (individual gauge for localized orbitals)[9] and GIAO (gauge including atomic orbitals),[10] evaluated the absolute NMR chemical shielding at the self-consistent field (SCF), level, newer developments are based on Møller–Plesset perturbation theory (GIAO-MP2, GIAO-MP3, and GIAO-MP4),[11] coupled cluster theory,[12] and density functional approaches (e.g., deMon-KS/deMon-NMR).[13]

For a number of amino acid residues the change in the NMR chemical shieldings with respect to ϕ and ψ (the ''NMR chemical shielding surfaces'') has already been obtained at the Hartree–Fock (HF) level.[14–16] The model systems employed for these computations are either *N*-acetyl-*N*′-methylamino acid amide or the smaller *N*-formylamino acid amide, for example, for alanine the two possible model systems would be *N*-acetyl-*N*′-methylalaninamide and *N*-formylalaninamide. Generally, a good correlation between computed and experimental shifts is found for C^{α}, C^{β}, and N with both model systems; but the change in the NMR chemical shielding of C′ cannot be reproduced based on ϕ and ψ only. Sulzbach et al.[17] showed that electron correlation cannot be the cause. The change in the absolute NMR chemical shielding due to correlation is nearly the same for different conformers on the (ϕ, ψ)-NMR chemical shielding surface. The same should be true for the rovibrational contributions that should be very similar for both the α-helical and the sheetlike structures.[18] Consequently, the influence of a nonplanar amide moiety on the chemical shielding of C′,[19] a different degree of hydrogen bonding,[20] or a combination of both are thought to be responsible for the disagreement between the computed and the experimental difference in the NMR chemical shieldings between an α-helix and a *β*-pleated sheet. The shielding surfaces obtained thus far were all computed for geometries that contain a planar or nearly planar amide group in each individual geometry.

A nonplanar distortion of an amide group is known to cause a large downfield shift of C′.[21] Hence, the correct description of the degree of nonplanarity of the amide group is imperative for the computation of the NMR chemical shielding of C′. All geometries employed in previous NMR chemical shift computations were obtained from empirical force field programs,[15] from X-ray structures,[14] or from *ab initio* optimizations at the restricted HF (RHF)/3–21G level of theory.[16] Empirical force fields penalize a nonplanar amide and predict the energy surface to be to steep.[22] X-ray crystallography is generally unable to determine the hydrogen atom positions. The 3–21G basis set is not flexible enough and seriously underestimates the degree of pyramidality of tricoordinate nitrogen compounds.[23,24] Consequently, we investigated the use of Becke3LYP/DZ*d* optimized geometries for the computation of the chemical shifts. We choose *N*-acetyl-*N*′-methylalaninamide (**1**) as the dipeptide model because the minima on the potential energy surface of **1** had been determined by a previous *ab initio* study[25] and a part of the (ϕ, ψ) shielding surface of C^{α} and C^{β} had been published by de Dios et al.[15] so that a comparison was possible.

Methods and Computational Details

All *ab initio* geometry optimizations as well as all geometry optimizations with density functional methods were carried out using the Gaussian 92/density functional theory (DFT) and Gaussian 94 packages.[26] The standard 3–21G basis set[27] and the double-zeta (DZ) C ($9s5p/4s2p$), H ($4s/2s$) basis set of Huzinaga[28] in Dunning's contraction[29] were employed. The DZ basis was augmented with a set of five spherical *d*-polarization functions on carbon (orbital exponent $\alpha_d = 0.75$) (DZ*d* basis set). To compute the NMR chemical shielding with DFT, the program combination deMon-KS/deMon-NMR with a modified IGLO type III basis set was employed.[9,13] The abbreviation deMon-KS shows that the Kohn–Sham functional

as implemented in the deMon package was used. For a more detailed discussion of the deMon-KS/deMon-NMR method see ref. 13. Malkin et al. showed that deMon-NMR predicts quite well the chemical shifts for which electron correlation is important.[13,30] The error margin is somewhat larger than at GIAO-MP2, but smaller than at GIAO-SCF.[13] Gaussian 94 was used to compute the chemical shifts at GIAO-SCF for both a modified triple-zeta (TZ) (9*s*5*p*/5*s*3*p*), H (5*s*/3*s*) basis set of Huzinaga[28] in Dunning's contraction[31] as implemented in Tx90[10b] and for the IGLO type III basis set that was employed to compute the chemical shifts at the DFT level. deMon-KS/deMon-NMR requires only moderate computational resources. Table I shows that the absolute chemical shielding differs strongly at GIAO-SCF and deMon-KS/deMon-NMR. For nuclei for which the effects of electron correlation are known to be small, the relative difference in the chemical shielding between GIAO-SCF/TZ and deMon-KS/deMon-NMR are in good agreement. If the GIAO-SCF calculations are carried out for the much larger, highly uncontracted IGLO III basis set, the chemical shieldings for atoms for which electron correlation is important are in much better agreement with the DFT results. However, a GIAO-SCF calculation that employed the IGLO III basis set took about 48 h on an IBM/590 workstation compared to 5 h for the DFT shifts. deMon-KS/deMon-NMR was employed in this study, because it gives equivalent or even better results (compare ref. 13 and references therein) at a much reduced computational cost.

We fully optimized the five lowest lying minima on the potential energy surface of **1** and compared the Becke3LYP/DZ*d* geometries and energies with those obtained at other levels of theory. The starting geometries for these structures were obtained from the RHF/3−21G energy surface for *N*-formylalaninamide (**2**).[22]

To construct the (ϕ, ψ) NMR chemical shielding surfaces, the chemical shielding was computed at each 60° gridpoint ϕ and ψ with the density functional program deMon-KS/deMon-NMR[13] for a Becke3LYP/DZ*d* optimized geometry. In the regions that correspond to the α helix and to the β-pleated sheet, a finer 30° grid was applied.

The calculations were carried out on IBM RS-6000 workstations at the Center for Computational Quantum Chemistry, the University of Georgia (Athens, GA). A typical geometry optimization (Becke3LYP/DZ*d*) took 30 h on an IBM/590 workstation.

TABLE I.
Comparison of NMR Chemical Shifts Computed for *N*-Acetyl-*N′*-Methylalaninamide (1).

	deMon-NMR/IGLO III			GIAO-SCF/TZ			GIAO-SCF/IGLO III			Difference		
Atom[a]	σ^{α}	σ^{β}	$\Delta\delta$	σ^{α}	σ^{β}	$\Delta\delta$	σ^{α}	σ^{β}	$\Delta\delta$	$\Delta\Delta\delta$ (A − B)	$\Delta\Delta\delta$ (A − C)	$\Delta\Delta\delta$ (B − C)
N^4	109.7	108.1	−1.7	142.6	140.4	−2.2	136.2	134.3	−1.9	0.5	0.2	−0.3
C^6 (C^{α})	121.6	128.4	6.8	149.3	154.0	4.7	138.5	143.5	5.0	2.1	1.8	−0.3
C^7 (C^{β})	162.1	162.1	0.0	181.2	180.1	−1.1	172.2	171.0	−1.2	1.1	1.2	0.1
C^9 (C')	8.7	8.7	0.0	4.3	3.7	−0.6	3.1	2.7	−0.4	0.6	0.4	−0.2
O^{10}	−88.2	−26.8	61.4	−161.3	−77.9	83.4	−94.3	−23.0	71.3	−22.0	−9.9	12.1

Absolute chemical shielding σ for the α-helix-like geometry (σ^{α}, $\phi = -60°$, $\psi = -60°$) and the β-pleated sheetlike geometry (σ^{β}, $\phi = -120°$, $\psi = 120$); difference in the chemical shifts between the α helix and the β-pleated sheet ($\Delta\delta$); relative difference between $\Delta\delta$ for deMon-NMR and $\Delta\delta$ for GIAO-SCF/TZ [$\Delta\Delta\delta$ (A − B)], between $\Delta\delta$ for deMon-NMR and $\Delta\delta$ for GIAO-SCF/IGLO basis III [$\Delta\Delta\delta$ (A − C)], and between $\Delta\delta$ for GIAO-SCF/TZ and $\Delta\delta$ for GIAO-SCF/IGLO basis III [$\Delta\Delta\delta$ (B − C)].

[a] For the atom numbering see Figure 3.

PARAMETERS USED TO DESCRIBE AMIDE MOIETY

We were particularly interested in the effect of a nonplanar amide group on the chemical shifts. The conventional way to assess the bending of the amide group is via ω. Head–Gordon et al. pointed out that even at RHF/3–21G ω can deviate by as much as 40° from 180°, e.g., to releave strain or to improve hydrogen bonding.[23] However, ω is close to 180° for most conformers. A major objection to the exclusive use of ω as a measure of the nonplanarity of the amide group is that pure twisting is not the only motion that can lead to nonplanarity. Out of plane bending of the three bonds attached to C′ or N, as pointed out by Ramachandran and Sasisekharan,[32] can also give a nonplanar amide moiety. As a consequence, we defined the bending of the amide groups in **1** in terms of the improper torsional angles χ_{C3}, χ_{N4}, χ_{C9}, and χ_{N11}. χ_{C3} is defined as the angle between the Me^1–C^3–N^4 plane and the O^2—C^3—N^4 plane, χ_{N4} as the angle between the C^3—N^4—C^6 plane and the C^3—N^4—H^5 plane, χ_{C9} as the angle between the C^6—C^9—N^{11} plane and the O^{10}—C^9—N^{11} plane, and χ_{N11} as the angle between the C^9—N^{11}—Me^{13} plane and the C^9—N^{11}—H^{12} plane (see Fig. 3).

As a third independent parameter for each amide moiety, the twist angle τ was defined as the angle between the bisectors of χ_C and χ_N as proposed by Winkler and Dunitz (Fig. 4).[33] Hence, τ_3 describes the twist of the π bond at C^3—N^4 and τ_9 the twist at C^9—N^{11}.

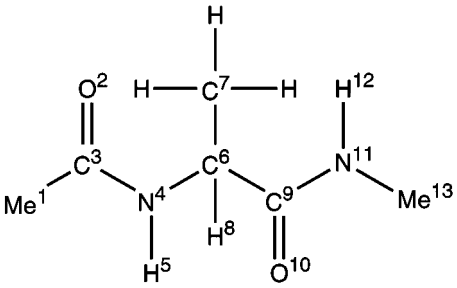

FIGURE 3. Atom numbering scheme for *N*-acetyl-*N*′-methylalanineamide (**1**). The improper torsional angle χ_{C3} is defined as the angle between the Me^1—C^3—N^4 and the O^2—C^3—N^4 planes, χ_{N4} as the angle between the C^3—N^4—C^6 and the C^3—N^4—H^5 planes, χ_{C9} as the angle between the C^6—C^9—N^{11} and the O^{10}—C^9—N^{11} planes and χ_{N11} as the angle between the C^9—N^{11}—Me^{13} and the C^9—N^{11}—H^{12} planes.

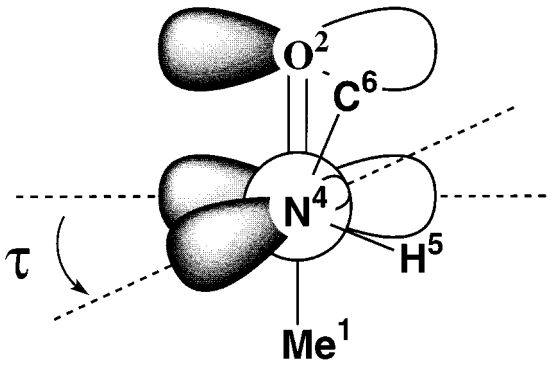

FIGURE 4. Definition of the twist angle τ shown for the C^3—N^4 bond. The magnitude of τ (which is the angle between the bisectors of χ_C and χ_N) reflects the amount by which the amide π-bond is twisted.

LOW ENERGY CONFORMERS OF *N*-ACETYL-*N*′-METHYLALANINAMIDE (1)

Due to the size of dipeptide model systems, the HF level has long been the only *ab initio* method that could be applied for the optimization of these molecules. Density functional methods, which have become practicable recently, are also capable of computing large systems. The density functional (Becke3LYP) results for glycine agree well with those of *ab initio* methods including electron correlation,[34] but to our knowledge no DFT studies on dipeptide models have been published. To evaluate the performance of Becke3LYP/DZ*d* for the optimization of peptide systems, we optimized the five lowest minima of **1** that are known from previous studies of *N*-acetyl-*N*′-methylalaninamide (**1**)[25] and *N*-formylalaninamide (**2**).[22] The locations of these minima, which are not restricted to the low energy regions of the Ramachandran plot, are shown in Figure 2. In Table II we compare their relative energies and (ϕ, ψ) values at the RHF/3–21G, Becke3LYP/DZ*d*, and RHF/DZP levels of theory. The corresponding structures are depicted in Figure 5.

The agreement in energies between RHF/3–21G and Becke3LYP/DZ*d* was surprisingly much better than that between the latter and RHF/DZP. The difference in the relative energies between Becke3LYP/DZ*d* and RHF/3–21G was less than 0.25 kcal/mol for $\mathbf{C7_{eq}}$, $\mathbf{C5}$, $\mathbf{C7_{ax}}$, and α_L and 0.6 kcal/mol for β_2. The RHF/DZP energies deviate between 0.3 kcal/mol ($\mathbf{C7_{ax}}$) and 1.4 kcal/mol (α_L) from the Becke3LYP/DZ*d* results. The agreement of the published MP2/TZVP//HF/6–31G**[25] energies for $\mathbf{C7_{eq}}$, $\mathbf{C_5}$, and $\mathbf{C7_{ax}}$ with the Becke3LYP/DZ*d* results was better with a maximum difference of 0.7 kcal/mol for $\mathbf{C7_{ax}}$.

TABLE II.
Location and Relative Energy of Five Lowest Minima of *N*-Acetyl-*N′*-Methylalaninamide (1) at RHF / 3–21G and Becke3LYP / DZ*d* and Comparison with RHF / DZP.

	RHF / 3–21G			Becke3LYP / DZ*d*			RHF / DZP[a]		
	ϕ	ψ	Energy	ϕ	ψ	Energy	ϕ	ψ	Energy
$C7_{eq}$	−85.8	69.0	0.00	−82.3	76.8	0.00	−85.9	79.1	0.0
C5	−167.0	169.0	1.13	−158.9	163.5	1.28	−156.0	161.0	0.5
$C7_{ax}$	74.4	−58.1	2.81	73.6	−61.2	2.72	75.8	−58.9	3.0
β_2	−127.6	27.8	3.61	−123.7	17.9	3.00	—	—	—[b]
α_L	63.4	32.8	5.80	72.1	18.2	5.81	65.9	33.5	4.4

[a] RHF / DZP results from ref. 25.
[b] β_2 has not been previously studied at this level.

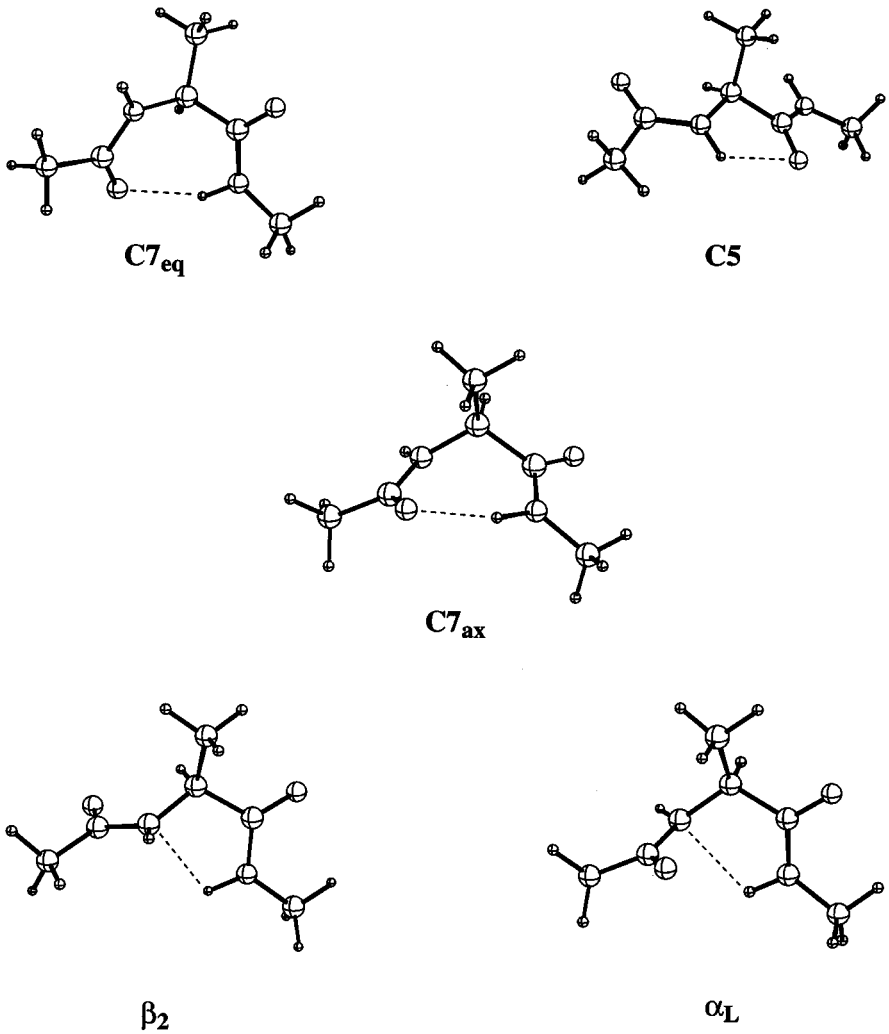

FIGURE 5. Qualitative molecular structures of the five low-energy conformations $C7_{eq}$, **C5**, $C7_{ax}$, β_2 and α_L of *N*-acetyl-*N′*-methylalanineamide (**1**).

TABLE III.
Absolute Deviations from Ideal Values for Parameters Describing Amide Group.

	RHF / 3–21G						Becke3LYP / DZ*d*					
	χ_{C3}	χ_{N4}	τ_{N4}	χ_{C9}	χ_{N11}	τ_{N11}	χ_{C3}	χ_{N4}	τ_{N4}	χ_{C9}	χ_{N11}	τ_{N11}
$\mathbf{C7_{eq}}$	0.2	0.5	4.4	0.0	3.6	0.4	0.9	6.2	4.1	0.3	16.4	2.3
C5	0.1	2.2	0.1	1.1	0.9	2.0	0.2	6.8	1.0	1.3	0.4	2.4
$\mathbf{C7_{ax}}$	0.5	1.0	4.8	2.4	1.1	1.1	0.5	0.8	4.8	2.5	7.3	1.9
β_2	0.3	15.0	0.5	2.1	2.3	1.6	1.1	23.4	0.2	1.3	8.8	0.9
α_L	0.3	14.4	0.2	5.1	7.3	1.9	0.7	22.5	3.6	5.7	19.6	3.3

Head–Gorden et al.[22] found that some of the structures of **2** with constrained ϕ and ψ values showed large deviations of ω from 180° and moderate deviations for χ_C. For structures with energetically unfavorable conformations, a ''trade-off'' (see below) between the energy required to distort from peptide planarity and the energy gained in maintaining favorable electrostatic interactions was found. Table III summarizes χ_C, χ_N, and τ for the five minima at both RHF/3–21G and Becke3LYP/DZ*d*. Even at RHF/3–21G small deviations from the ideal values of χ_C, χ_N, and τ exist.

The nonideal values for χ_C, χ_N, and τ can be rationalized as a consequence of improved electrostatic interactions: while the backbone dihedrals change to reduce steric strain, the hydrogen of the amide group ''follows'' the oxygen or nitrogen atom to which it is hydrogen bonded to maintain the best bond length. In $\mathbf{C7_{eq}}$ and $\mathbf{C7_{ax}}$, the two minima in which hydrogen bonding leads to a seven-membered ring structure, only χ_{N11} of the Becke3LYP/DZ*d* structure of $\mathbf{C7_{eq}}$ deviates significantly from 180° ($\Delta\chi_{N11}$ = 16.4°). The deviation is paralleled by a change in ψ from 69° at RHF/3–21G to 77° at Becke3LYP/DZ*d* (Table II), while the length of the O···H bond changes very little (2.029 vs. 2.070 Å). Figure 6 shows that less energy is required to distort an amide group from planarity at Becke3LYP/DZ*d*. Consequently, the unfavorable steric interaction between H^5 and C^7 and between O^{10} and C^7 in structure $\mathbf{C7_{eq}}$ is reduced by increasing ψ. To maintain the ideal hydrogen bonding distance, the dihedral angle χ_{N11} and to a lesser degree χ_{N4} ($\Delta\chi_{N4}$ = 6.2°) change in order to keep O^2 and H^{12} close together. In $\mathbf{C7_{ax}}$, C^7 is in an axial position and does not interact strongly with H^5 and O^{10}. A change in ψ or ϕ to relieve strain is not necessary. Consequently, χ_N is close to 180° and ϕ as well as ψ are nearly the same at both HF and DFT. **C5** is stabilized by an interaction between H^5 and O^{10} that leads to a five-membered ring structure. The hydrogen bond is in plane with the amide group and a nonplanar amide cannot affect the O···H distance. Hence, ϕ and ψ at RHF/3–21G and Becke3LYP/DZ*d* agree with χ_N is close to 180°.

The remaining two structures, β_2 and α_L, are stabilized by hydrogen bonding between H^{12} and the amide nitrogen N^4 (Fig. 5). This interaction leads to a tetracoordinate N^4 and causes χ_{N4} to deviate by about 15° from 180°, even in the RHF/3–21G optimized structures of β_2 and α_L. At Becke3LYP/DZ*d* the effect is more pronounced with a $\Delta\chi_{N4}$ of about 23°. In addition, χ_{N11} in α_L deviates by about 20° from 180°. Again, the change in $\Delta\chi_N$ is accompanied by changes in ϕ and ψ at the HF and density functional levels (Table II).

The above results for the five minima of **1** show that the Becke3LYP/DZ*d* method is well suited to model peptide systems. The RHF/3–21G relative

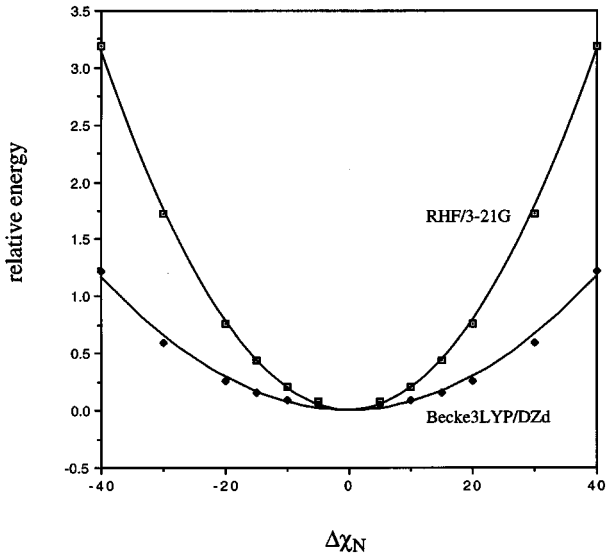

FIGURE 6. Change in the relative energy (kcal / mol) of *N'*-methylformamide with respect to increasing $\Delta\chi_N$ (degrees) at RHF / 3–21G and Becke3LYP / DZ*d*. $\Delta\chi_N$ is the angle between the Me — N — C′ and the H — N — C′ planes in *N*-methyl-acetylamide (**3**).

energies are in surprisingly good agreement with those of Becke3LYP/DZ*d*. The agreement of Becke3LYP with the MP2 single point energies is also good and might improve further if the energies were computed for MP2 optimized structures, which should have a less planar amide group. DFT and MP2 predict the trade-off for a nonplanar amide moiety to be much smaller than predicted by HF theory. (The tendency of MP2 to yield a less planar nitrogen environment is shown in ref. 19.) The larger $\Delta\chi_N$ values are accompanied by changes in ϕ and ψ. Hence, the simple RHF/3−21G method is sufficient to obtain rough energy surfaces of model dipeptides and to locate minima, but Becke3LYP/DZ*d* reproduces hydrogen-bonded structures more accurately.

INFLUENCE OF CHANGES IN χ_C, χ_N, AND τ ON CHEMICAL SHIFTS OF C′, C$^\alpha$, AND N

In the previous section we showed that at Becke3LYP/DZ*d* χ_N, χ_C, and τ of the five minima structures deviate from the ideal values of 180° (χ_N and χ_C) and 0° (τ). Numerous steric interactions and hydrogen bonds exist in larger peptides. In these systems the ability of the amide moiety to trade-off planarity to improve electrostatic interactions or to reduce steric strain while maintaining good hydrogen-bonding distances is very important. Sizable deviations of χ_N and smaller changes for of χ_C and τ from their values in a planar amide can be expected, a fact pointed out by Winkler and Dunitz based on their studies of cyclic lactams.[33] $\Delta\chi_N$ affects the chemical shift of C′, which has been shown both theoretically and experimentally.[19,21] To explore the dependence of the chemical shifts of C′, C$^\alpha$, and N on the nonplanarity of the amide moiety quantitatively, we computed the chemical shifts for 25 partially optimized structures of *N*-methylacetyl amide (**3**) with constrained values of χ_N, χ_C, and τ. All other geometrical parameters were optimized at Becke3LYP/DZ*d*. Table IV summarizes the changes in the absolute chemical shifts of C′, C$^\alpha$, and N ($\Delta\delta$ ^{13}C C′, $\Delta\delta$ ^{13}C C$^\alpha$, and $\Delta\delta$ ^{15}N N)

TABLE IV.
Relative Changes of Absolute Chemical Shielding of C′, C$^\alpha$, and N in *N*-Methylacetamide (3) with Respect to $\Delta\chi_N$, $\Delta\chi_C$, and $\Delta\tau$.

$\Delta\chi_N$	$\Delta\chi_C$	$\Delta\tau$	δ ^{13}C C′	δ ^{13}C C$^\alpha$	δ ^{15}N N
0	0	0	0.00	0.00	0.00
10	0	0	−0.38	−0.18	−0.04
20	0	0	−1.65	−0.88	0.09
0	0	5	−0.20	−0.16	0.65
10	0	5	−0.57	−0.25	0.20
20	0	5	−1.87	−1.06	0.09
30	0	5	−4.22	−2.45	−0.24
0	0	10	−0.81	−0.53	1.70
10	0	10	−1.14	−0.72	1.28
20	0	10	−2.54	−1.51	0.63
30	0	10	−4.63	−3.01	0.21
40	0	10	−6.89	−4.02	−0.38
0	5	10	−0.64	−0.59	2.15
10	5	10	−0.98	−0.71	1.90
20	5	10	−2.43	−1.35	1.40
30	5	10	−4.20	−2.72	0.62
40	5	10	−6.69	−3.80	0.25
0	10	10	−1.24	−0.63	1.76
10	10	10	−1.61	−0.71	1.58
20	10	10	−2.68	−1.23	1.51
30	10	10	−4.50	−2.47	1.55
40	10	10	−7.00	−3.45	1.25
20	10	15	−3.12	−2.43	2.75
30	10	15	−4.79	−2.92	2.35
40	10	15	−7.22	−3.86	2.27

The changes in the shielding are with respect to the chemical shielding in a perfectly planar amide.

computed with deMon-NMR, together with the corresponding values of $\Delta\chi_N$, $\Delta\chi_C$, and $\Delta\tau$.

An evaluation of the data in Table IV shows that $\Delta\delta\,^{13}$C C′ can be reproduced with a R^2 value of 0.99 and a root mean square error of only 0.2 ppm with eq. (1).[35]

$$\Delta\delta\,^{13}\mathrm{C}\,\mathrm{C}' = +0.1199 - 91.9*10^{-3}\Delta\tau - 19.6*10^{-3}\Delta\chi_N - 3.3*10^{-3}\Delta\chi_N^2. \quad (1)$$

The dependence of $\Delta\delta\,^{13}$C C′ on $\Delta\chi_C$ is not statistically significant. Its inclusion does not improve the agreement between the theoretical result and $\Delta\delta\,^{13}$C C′ obtained from eq. (1). Because $\Delta\chi_C$ is expected to be small in unconstrained peptides (compare Table II), it was omitted from eq. (1). Figure 7 shows that the change in the chemical shift of C′ computed with eq. (1) is in excellent agreement with the theoretical results.

The α carbon in peptides is adjacent to two amide moieties. It is connected to the first via the nitrogen and to the second via the carbonyl carbon. The *N*-methyl group in **3** corresponds to the nitrogen linked side of C^α and the methyl of the acetyl group in **3** corresponds to the C′ linked side of the α carbon. We find only a very small dependence of the methyl group bound to C′ (C^{acetyl}) in **3** on χ_N, χ_C, and τ. The difference between the largest and smallest value of $\delta\,^{13}$C C^{acetyl} is only 0.8 ppm. Therefore, in the following discussion, C^α in **3** refers to the *N*-methyl group. The chemical shift of the carbon atom of the *N*-methyl group changes over a range of 4 ppm due to τ and χ_N. Equation (2) shows the change of ^{13}C C^α as a function of $\Delta\tau$ and $\Delta\chi_N$. As for C′, the influence of $\Delta\chi_C$ is not statistically significant for the reproduction of $\Delta\delta\,^{13}$C C^α and the same arguments apply.

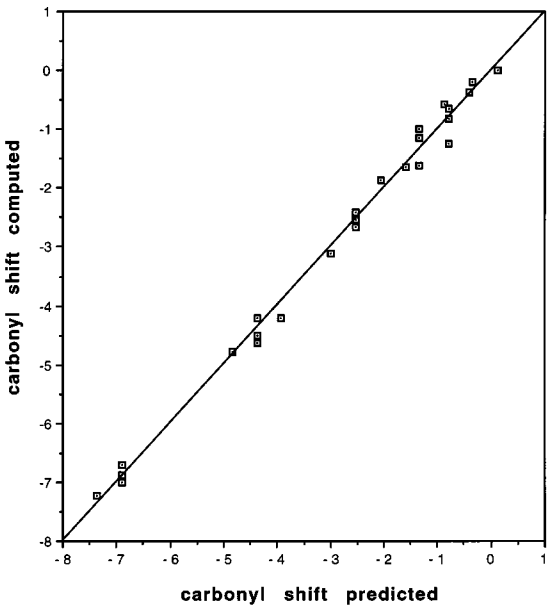

FIGURE 7. Change in the chemical shielding of the carbonyl carbon in (**3**) with respect to $\Delta\tau$ and $\Delta\chi_N$. The change in the theoretical shielding (deMon-NMR/IGLO-basis III) is plotted on the vertical axis, and the change in the shielding derived with equation 1 on the horizontal axis.

$$\Delta\delta\,^{13}\mathrm{C}\,\mathrm{C}^\alpha = +0.1874 - 69.7*10^{-3}\Delta\tau - 21.4*10^{-3}\Delta\chi_N - 1.5*10^{-3}\Delta\chi_N^2. \quad (2)$$

The R^2 value for eq. (2) is 0.97 and the root mean square error is 0.25 ppm. This demonstrates that the chemical shift of C^α is also affected by a nonplanar amide group. A strongly nonplanar amide group can deshield C^α by up to 4 ppm!

The situation is more complex for the amide nitrogen. Both $\Delta\tau$ and $\Delta\chi_C$ increase the shielding of the nitrogen atom, while $\Delta\chi_N$ deshields it. The net effect on the chemical shielding is small. Equation (3) reproduces the theoretical result for $\Delta\delta\,^{15}$N of the amide nitrogen with an R^2 value of 0.91 and a root mean square error of 0.29 ppm.

$$\Delta\delta\,^{15}\mathrm{N}\,\mathrm{N}^{amide} = +0.4061 + 1.0*10^{-3}\Delta\tau^2 + 84.0*10^{-3}\Delta\chi_C - 33.6*10^{-3}\Delta\chi_N. \quad (3)$$

Our data demonstrate that the chemical shifts of C′ and C^α depend strongly on $\Delta\chi_N$ and moderately on τ. To obtain the change in the shielding due to ϕ and ψ only, the effect of the nonplanar amide moiety on the chemical shifts has to be eliminated.

SHIELDING SURFACES CORRECTED FOR INFLUENCE OF AMIDE NONPLANARITY

Until now, the dependence of the chemical shifts of the various backbone atoms on a nonplanar amide group has not been taken into account. Clearly, the shielding surface of C′, C^α, and N with respect to ϕ and ψ will contain contributions due to $\Delta\chi_C$, $\Delta\chi_N$, and $\Delta\tau$. While the change in the chemical shielding caused by $\Delta\chi_C$, $\Delta\chi_N$, and $\Delta\tau$ should be similar at all levels of theory, the magnitude of $\Delta\chi_C$, $\Delta\chi_N$, and $\Delta\tau$ itself varies for different levels of theory. Becke3LYP/DZ*d* predicts softer bending modes for the amide moiety and consequently larger values for $\Delta\chi_C$, $\Delta\chi_N$, and $\Delta\tau$ than, for example, RHF/3−21G (compare Table II).

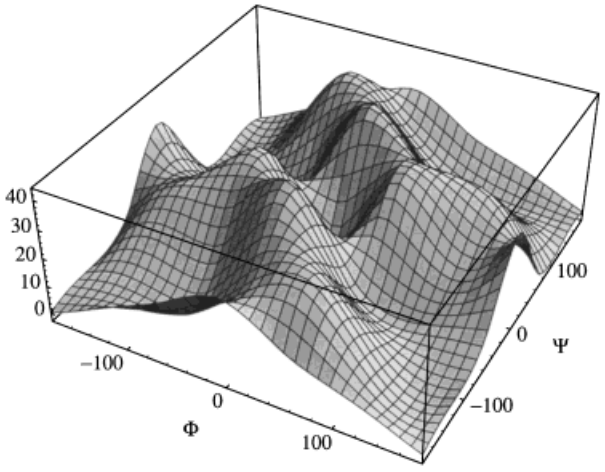

FIGURE 8. 3-D-Plot of $\Delta\chi_{N11}$ (z-axis) with respect to ϕ and ψ based on a 60° grid. To obtain a smooth surface, additional data-points were interpolated. χ_{N11} is the angle between the $C^9 — N^{11} — Me^{13}$ plane and the $C^9 — N^{11} — H^{12}$ plane. $\Delta\chi_{N11}$ is the deviation of χ_{N11} from 180°.

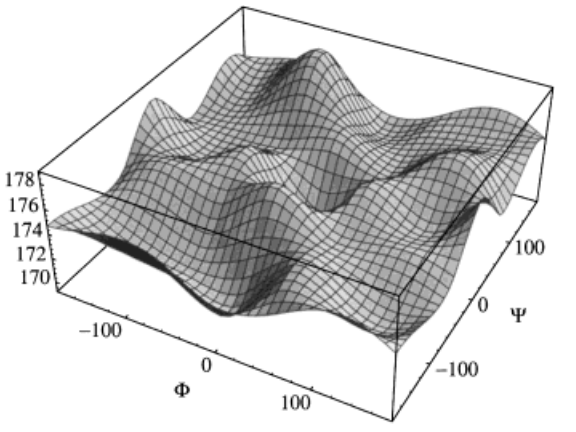

FIGURE 9. 3-D Plot of the (ϕ, ψ)-shielding surface of C′ which still contains contributions due to $\Delta\chi_{N11}$ and $\Delta\tau_{N11}$. The z-axis shows the relative chemical shielding of C′ with respect to TMS computed at the same level. To obtain a smooth surface additional data-points were interpolated.

This causes the chemical shifts based on Becke3LYP optimized geometries to contain larger contributions due to the nonplanar amide group. This effect is most pronounced for δ ^{13}C C′ which depends strongly on $\Delta\chi_N$. Figure 8 shows the (ϕ, ψ) surface of $\Delta\chi_{N11}$.

$\Delta\chi_{N11}$ has the largest effect on δ ^{13}C C′. The average value for $\Delta\chi_{N11}$ is 17.4° and the largest deviation from 180° which is found for the (0°/60°) and the (0°/ − 60°) geometries is 42°! The origin for this large deviation was first discussed by Head−Gordon et al.[22] The (0°/0°) structure suffers from severe steric strain but is stabilized by a seven-membered ring which causes $\Delta\chi_{N11}$ to be only 2°. The (0°/60°) and the (0°/ − 60°) structures experience less steric strain, but they also lose most of the stabilizing hydrogen-bonding interaction of the (0°/0°) structure. To recover some of the favorable electrostatic interaction the hydrogen atom ''follows'' the oxygen atom, thereby bending the amide moiety ($\chi_N \approx 40°$). While 40° is the largest value of $\Delta\chi_{N11}$ in this study, Figure 8 shows that many other geometries also have sizable $\Delta\chi_{N11}$ values. A shielding surface for C′ which is constructed from the uncorrected theoretically derived shifts should contain large contributions due to $\Delta\chi_{N11}$ and $\Delta\tau_9$. To obtain the NMR chemical shielding surface of C′ based only on ϕ and ψ, the contributions of $\Delta\chi_{N11}$ and $\Delta\tau_9$ on δ ^{13}C C° have to be computed for each structure on the surface by means of eq. (1), and the result has to be subtracted from the computed absolute shielding. Figure 8 shows $\Delta\chi_{N11}$ as a function of ϕ and ψ. Figures 9 and 10 show the shielding surface of C′ before (Fig. 9) and after (Fig. 10) the contributions of $\Delta\chi_{N11}$ and $\Delta\tau_9$ have been subtracted. A comparison of Figures 8, 9, and 10 shows that the NMR chemical shielding surface of C′ that has not been corrected by eq. (1) is dominated by contributions due to $\Delta\chi_{N11}$ (and $\Delta\tau_9$) rather than by ϕ and ψ.

For C^α the effect of $\Delta\chi_{N4}$ on ^{13}C is up to 4 ppm for $\Delta\chi_{N4} = 40°$. The change in δ ^{13}C C^α due to ϕ

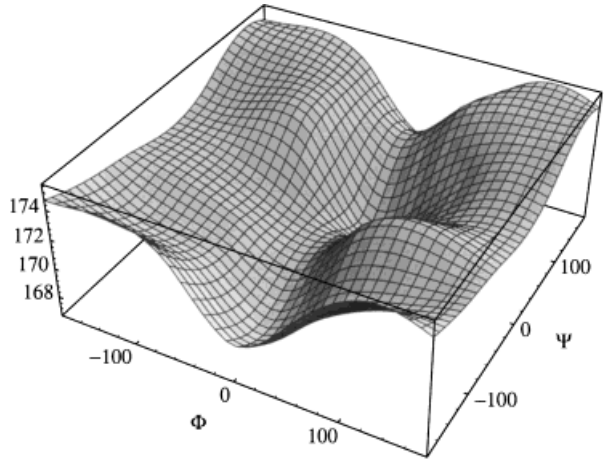

FIGURE 10. 3-D Plot of the (ϕ, ψ)-shielding surface of C′ corrected for the effects of $\Delta\chi_{N11}$ and $\Delta\tau_{N11}$. The z-axis shows the relative chemical shielding of C′ with respect to TMS computed at the same level. To obtain a smooth surface additional data-points were interpolated.

and ψ is larger than that caused by $\Delta\chi_{N4}$ and $\Delta\tau_3$, but eq. (2) should still be used to eliminate the influence of $\Delta\chi_{N4}$ and $\Delta\tau_3$ on $\delta\,^{13}C\,C^{\alpha}$.

The corrected shielding surface of C^{α} is in good agreement with the $\delta\,^{13}C\,C^{\alpha}$ surface computed by de Dios et al.,[15] who employed the empirical force field program Discover (Biosym Technologies, San Diego, CA) to obtain the geometries used for the calculation of the NMR chemical shifts. In their study only ϕ and ψ were varied, while all other geometrical parameters remained frozen. Consequently, the results of de Dios et al. did not contain contributions due to $\Delta\chi_N$ and $\Delta\tau$. For C^{β}, which should not be affected by a nonplanar amide group, our shielding surface also agrees well with that of de Dios et al.

Figure 11 shows a contour plot of the corrected [with eq. (3)] shielding surface for the amide nitrogen (N^4) with respect to ϕ and ψ for a 30° grid in the region of the α helix and the β-pleated sheet and a 60° grid elsewhere. To our knowledge, no such surface has been published previously. The location and absolute height of the extrema might change slightly when a finer grid is applied, but the overall range of the chemical shielding of about 26 ppm, which is remarkably large, should remain the same. The result is particularly valuable, because the surface is very steep in the region of the α helix and the β-pleated sheet and small geometrical changes in those regions will result in $\Delta\delta\,^{15}N$ values of several parts per million. Once an initial structure for a protein was obtained, the shielding surface of the amide nitrogen surface allowed the determination of the theoretical chemical shieldings for the various alanine amide nitrogen atoms in the protein. Minimization of the difference between the theoretical and the experimental shift values should allow the refinement of the protein structure. This method was already applied successfully in the case of C^{α} and C^{β}.[36]

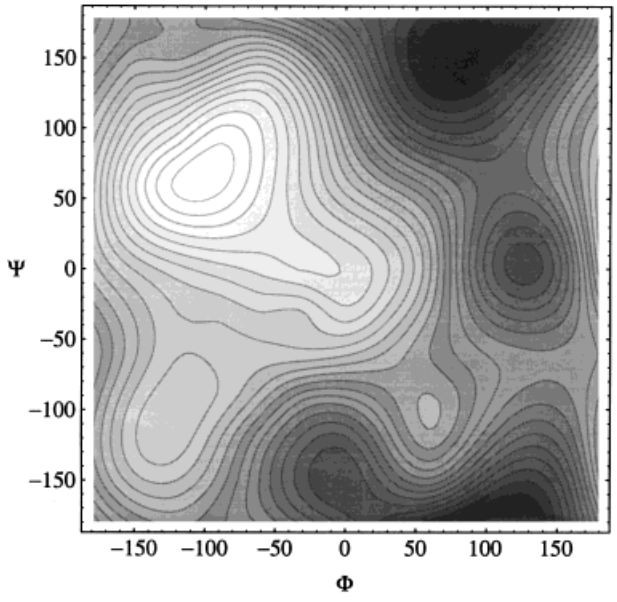

FIGURE 11. Countour plot of the (ϕ, ψ)-shielding surface of N^4 corrected for the effect of a nonplanar amide nitrogen. The contour lines are separated by one ppm. $\Delta\delta\,^{15}N\,N^4$, which is much larger than that for C′ or C^{α} ranges from −236 ppm (−120°/60°) to −262 ppm (120°/180°) on the NH_4NO_3 scale.

Studies of a large number of amino acid residues with known ϕ and ψ values gave evidence of the existence of an empirical correlation between the conformation and the chemical shifts. Typically, C^{α} and C′ experience a downfield shift in an α helix and an upfield shift in a β-pleated sheet. Also, C^{β} resonances are shifted upfield in an α helix and downfield in a β strand.[5–7] If we as-

TABLE V.
Computed and Experimental Difference in Chemical Shielding Between an α Helix and a β-Pleated Sheet.

	Calculated Values			Experimental Data		
Atom	δ_α	δ_β	$\Delta\delta = \delta_\alpha - \delta_\beta$	Ref. 5[a]	Ref. 7[b]	Ref. 6[c]
C^{α}	60.5	52.9	7.6	3.5 ± 0.3	3.5 ± 3.0	4.6 ± 2.2
C′	171.0	175.3	−4.3	4.6 ± 0.3	2.1 ± 4.0	—
C^{β}	21.2	22.9	−1.7	−4.8 ± 0.3	—	−2.5 ± 2.8
N	−244.5	−246.8	2.3	—	0.0 ± 4.0	—

[a] Solid-state NMR of homopolymers.
[b] NMR data of alanine residues in solution based on X-ray structures.
[c] NMR data of different residues in solution based on X-ray structures.

sume that these changes are only due to the different values of ϕ and ψ, our model will have to reproduce these trends. Our computed difference in the N and C^{β} chemical shifts between an α helix and a β-pleated sheet agrees well with the available experimental data (Table V). The computed $\Delta\delta$ for C^{α} is too large. The GIAO-SCF value of 4.1 ppm (data from Table I corrected for $\Delta\chi_N$ and $\Delta\tau$) agrees much better with the experimental data. For C′ $\Delta\delta$ does not agree with the experimental value at all. However, we have shown in the previous sections that χ_N is needed as a third parameter to describe the chemical shift of the carbonyl carbon. The restrained geometries and those of the five minima show that the improper torsional angle χ_N depends on the hydrogen-bonding environment of the amide group. The amide group can become highly nonplanar if this assists hydrogen bond formation.

Our computed results for C′ are in much better agreement with experimental data when $\Delta\chi_N$ of about 30° in the α-helical structures is assumed. However, more elaborate theoretical and experimental studies are needed to find out whether or not this is actually the case. Another possibility, discussed in detail by de Dios et al.,[20] is that the chemical shift of C′ is strongly affected by hydrogen bonding.

Conclusions

Density functional methods appear to be well suited for the theoretical evaluation of the optimization of peptide structures as well as for the computation of the NMR chemical shifts of dipeptide models. The relative stability of all the minima examined agrees well between Becke3LYP/DZ*d* and RHF/3−21G. Unlike RHF/3−21G, Becke3LYP/DZ*d* predicts soft modes for the out of plane bending of the amide group. Consequently, **C5** and $\mathbf{C7_{ax}}$, which have nearly planar amide groups at Becke3LYP/DZ*d*, can be reproduced at the RHF/3−21G level. For $\mathbf{C7_{eq}}$, β_2, and α_L, a nonplanar amide group results in increased hydrogen bonding or decreased steric interactions. Therefore, the optimized ϕ and ψ values for these minima differ by up to 14° between the two methods.

The NMR chemical shifts of C′ and C^{α} not only depend on ϕ and ψ, but also on the nonplanarity of the amide group. The dependence of $\delta\ ^{13}C\ C'$ and $\delta\ ^{13}C\ C^{\alpha}$ on the nonplanarity of the amide group is best described in terms of the improper torsional angles χ_N and χ_C and the angle τ that defines the bisector between χ_N and χ_C. A suitable correlation between $\Delta\chi_N$, $\Delta\chi_C$, and $\Delta\tau$ with $\Delta\delta\ ^{13}C\ C'$ and with $\Delta\delta\ ^{13}C\ C^{\alpha}$ can be obtained based on *N*-methyl-acetylamide as a model system. The parameters from this model allow shielding surfaces of C′ and C^{α} corrected for the influence of the nonplanar amide on C^{α} and C′ to be developed.

While the deMon-NMRs/IGLO-basis III/Becke3LYP/DZ*d* NMR-shielding surfaces for C^{β} and N are in good general agreement with available literature data, the computed $\Delta\delta\ ^{13}C\ C^{\alpha}$ differs from the experimental value by several parts per million. For our model system, which excludes 1,4-intramolecular, intermolecular hydrogen bonding, and other long-range effects, the GIAO-SCF/TZ result reproduces $\Delta\delta\ ^{13}C\ C^{\alpha}$ better. For the shielding surfaces of C′ (corrected for $\Delta\chi_N$ and $\Delta\tau$), the agreement with the experiment improves significantly if the amide moiety in the α helix is assumed to be nonplanar. However, the failure to compute $\delta\ ^{13}C\ C'$ correctly could be due to hydrogen bonding.

Acknowledgments

The authors thank Professor D. R. Salahub for providing them with a copy of deMon. The work in Erlangen was supported by the Deutsche Forschungsgemeinschaft, the Convex Computer Corporation, the Fonds der Deutschen Chemischen Industrie (fellowship for H.M.S.), and the Stiftung Volkswagenwerk. The work in Georgia was supported by the U.S. National Science Foundation.

References

1. (a) K. Wüthrich, *NMR of Proteins and Nucleic Acids*, New York, 1986; (b) G. Wagner, *Prog. NMR Spectrosc.*, **22**, 101 (1990).
2. D. Neuhaus and M. P. Williamson, *The Nuclear Overhauser Effect in Structural and Conformational Analysys*, VCH, New York, 1989.
3. T. E. Creighton, *Proteins Structures and Molecular Properties*, 2nd ed., Freeman, New York, 1993.
4. G. N. Ramachandran, C. Ramakrishnan, and V. Sasisekharan, *J. Mol. Biol.*, **7**, 95 (1963).
5. H. R. Kricheldorf and D. Müller, *Macromolecules*, **16**, 615 (1983).
6. S. Spera and A. Bax, *J. Am. Chem. Soc.*, **113**, 5490 (1991).
7. D. S. Wishart, B. D. Sykes, and F. M. Richards, *J. Mol. Biol.*, **222**, 311 (1991).

8. (a) D. Hnyk, E. Vajda, M. Bühl, and P. v. R. Schleyer, *Inorg. Chem.*, **31**, 2464 (1992); (b) M. Bühl and P. v. R. Schleyer, *J. Am. Chem. Soc.*, **114**, 477 (1992); (c) M. Bühl and P. v. R. Schleyer, *Struct. Chem.*, **4**, 1 (1993); (d) A. M. Mebel, O. P. Charkin, and P. v. R. Schleyer, *Inorg. Chem.*, **32**, 469 (1993); (e) D. D. Laws, A. C. de Dios, and E. Oldfield, *J. Biomol. NMR*, **3**, 607 (1993); (f) D. Jiao, M. Barfield, and V. J. Hruby, *Magn. Reson. Chem.*, **31**, 75 (1993); (g) D. B. Chestnut and C. G. Phung, *Chem. Phys. Lett.*, **183**, 505 (1991); (h) D. B. Chestnut and C. G. Phung, in *Nuclear Magnetic Shieldings and Molecular Structure*, J. A. Tossell Ed., Kluwer Academic Publishers, New York, 1993; (i) D. B. Chestnut, B. E. Rusiloski, K. D. Moore, and D. A. Egolf, *J. Comput. Chem.*, **11**, 1364 (1993).
9. (a) W. Kutzelnigg, *Isr. J. Chem.*, **19**, 193 (1980); (b) M. Schindler and W. Kutzelnigg, *J. Chem. Phys.*, **76**, 1919 (1982); (c) M. Schindler and W. Kutzelnigg, *J. Am. Chem. Soc.*, **105**, 1360 (1983); (d) U. Fleischer and M. Schindler, *Chem. Phys.*, **120**, 103 (1988); (e) W. Kutzelnigg, U. Fleischer, and M. Schindler, *NMR Basic Principles and Progress*, Vol. 23, Springer–Verlag, Berlin, 1990.
10. (a) R. Ditchfield and P. D. Ellis, in *Topics in Carbon-13 NMR Spectroscopy*, G. C. Levy, Ed., Wiley, New York, 1974; (b) P. Pulay, K. Wolinski, and J. F. Hinton, *J. Am. Chem. Soc.*, **112**, 8251 (1990), and references therein.
11. (a) J. F. Stanton, J. Gauss, J. D. Watts, W. J. Lauderdale, and R. J. Bartlett, *Int. J. Quantum Chem. Quantum Chem. Symp.*, **S26**, 879 (1992); (b) J. Gauss, *J. Chem. Phys. Lett.*, **191**, 614 (1992); (c) J. Gauss, *J. Chem. Phys.*, **99**, 3629 (1993); (d) J. Gauss, *J. Chem. Phys. Lett.*, **229**, 198 (1994).
12. J. Gauss and J. F. Stanton, *J. Chem. Phys.*, **102**, 251 (1995).
13. V. G. Malkin, O. L. Malkina, M. E. Casida, and D. R. Salahub, *J. Am. Chem. Soc.*, **116**, 5898 (1994).
14. A. C. de Dios, J. G. Pearson, and E. Oldfield, *Science*, **260**, 1491 (1993).
15. A. C. de Dios, J. G. Pearson, and E. Oldfield, *J. Am. Chem. Soc.*, **115**, 9769 (1993).
16. D. Jiao, M. Barfield, and V. J. Hruby, *J. Am. Chem. Soc.*, **115**, 10883 (1993).
17. H. M. Sulzbach, P. v. R. Schleyer, and H. F. Schaefer, *J. Am. Chem. Soc.*, **116**, 3967 (1994).
18. For a more detailed discussion of rovibrational effects on the chemical shielding see ref. 11c and also C. J. Jameson, *Chem. Rev.*, **91**, 1375 (1991).
19. H. M. Sulzbach, P. v. R. Schleyer, and H. F. Schaefer, *J. Am. Chem. Soc.*, **117**, 2632 (1995).
20. A. C. de Dios and E. Oldfield, *J. Am. Chem. Soc.*, **116**, 11485 (1994).
21. H. Shao, X. Jiang, P. Gantzel, and M. Goodman, *Chem. Biol.*, **1**, 231 (1994).
22. T. Head–Gordon, M. Head–Gordon, M. J. Frisch, C. L. Brooks, and J. A. Pople, *J. Am. Chem. Soc.*, **113**, 5989 (1991).
23. G. M. Wright, R. J. Simmonds, and D. E. Parry, *J. Comput. Chem.*, **9**, 601 (1988).
24. J. S. Kwiatkowski and J. Leszczyński, *J. Mol. Struct.*, **279**, 277 (1993).
25. (a) H.-J. Böhm and S. Brode, *J. Am. Chem. Soc.*, **113**, 7129 (1991); (b) I. R. Gould and P. A. Kollman, *J. Phys. Chem.*, **96**, 9255 (1992).
26. M. J. Frisch, G. W. Trucks, H. B. Schlegel, P. M. W. Gill, B. G. Johnson, M. A. Robb, J. R. Cheeseman, T. Keith, G. A. Petersson, J. A. Montgomery, K. Raghavachari, M. A. Al-Laham, V. G. Zakrzewski, J. V. Ortiz, J. B. Foresman, J. Cioslowski, B. B. Stefanov, A. Nanayakkara, M. Challacombe, C. Y. Peng, P. Y. Ayala, W. Chen, M. W. Wong, J. L. Andres, E. S. Replogle, R. Gomperts, R. L. Martin, D. J. Fox, J. S. Binkley, D. J. DeFrees, J. Baker, J. P. Stewart, M. Head–Gordon, C. Gonzalez, and J. A. Pople, *Gaussian 94, Revision C.3*, Gaussian, Inc., Pittsburgh, PA, 1994.
27. W. J. Hehre, L. Radom, J. A. Pople, and P. v. R. Schleyer, *Ab Initio Molecular Orbital Theory*, Wiley, New York, 1986.
28. S. Huzinaga, *J. Chem. Phys.*, **45**, 1293 (1965).
29. T. H. Dunning, *J. Chem. Phys.*, **53**, 2823 (1970).
30. (a) V. G. Malkin, O. Malkina, D. R. Salahub, and L. Erickson, in *Density Functional Theory, a Tool for Chemistry*, P. Politzer and J. Seminario, Eds., Elsevier, Amsterdam, 1995; (b) T. B. Woolf, V. G. Malkin, O. L. Malkina, D. R. Salahub, and B. Roux, *Chem. Phys. Lett.*, **239**, 186 (1995).
31. T. H. Dunning, *J. Chem. Phys.*, **55**, 716 (1971).
32. G. N. Ramachandran and V. Sasisekharan, *Adv. Protein Chem.*, **23**, 283 (1968).
33. F. K. Winkler and J. D. Dunitz, *J. Mol. Biol.*, **59**, 169 (1971).
34. V. Barone, C. Adamo, and F. Lelj, *J. Chem. Phys.*, **102**, 364 (1995).
35. JMP-in, SAS Institute Inc., Cary, NC. This program was employed for the statistical analysis, 1989.
36. J. G. Pearson, J.-F. Wang, J. L. Markley, H.-B. Le, and E. Oldfield, *J. Am. Chem. Soc.*, **117**, 8823 (1995) and references therein.